Iron–Formaldehyde Interaction: *'ab initio'* Calculations on the Model Compounds $[Fe(CO)_{4-n}(PH_3)_n(\eta^2\text{-}CH_2O)]$ (*n* = 0, 2, or 4)†

Marzio Rosi, Antonio Sgamellotti*, and Francesco Tarantelli
Dipartimento di Chimica, Università di Perugia, Via Elce di Sotto 8, I-06100 Perugia, Italy
Carlo Floriani
I.C.M.A., Université de Lausanne, Place du Château 3, CH-1005 Lausanne, Switzerland
Martyn F. Guest
Computational Science Group, SERC Daresbury Laboratory, Daresbury, Warrington WA4 4AD

'Ab initio' calculations have been performed on the model systems $[Fe(CO)_{4-n}(PH_3)_n(\eta^2\text{-}CH_2O)]$ (*n* = 0, 2, or 4), to investigate the nature and the energetics of the interaction between iron and formaldehyde. The results allow a complete description of the electronic structure of the model compounds: the bond between Fe and CH_2O may essentially be described in terms of the π-back donation from an occupied metal orbital, of mainly d_{xz} character, to the π* orbital of formaldehyde. Partial geometry optimizations obtained by gradient calculations show that the geometry of the co-ordinated CH_2O is greatly distorted and the distortion increases with the substitution of carbonyl ligands with phosphines. Configuration-interaction calculations, performed on the $[Fe(CO)_4(\eta^2\text{-}CH_2O)]$ system using the direct configuration-interaction approach, suggest that the interaction energies computed at the Hartree–Fock level are reliable.

The nature of the co-ordinate bond between a transition metal and a formaldehyde molecule is relevant due to the role played by the M–CH_2O functionality in carbon monoxide reduction.[1,2] This functionality has recently been studied both by experimentalists and theoreticians. While experimental studies have led to the synthesis and structural characterization of several CH_2O complexes, including those with osmium,[3] vanadium,[4] molybdenum,[5] rhenium,[6] and iron,[7] *'ab initio'* theoretical studies appear limited to a single species, the nickel complex $[Ni(PH_3)_2(CH_2O)]$.[8] This latter work demonstrated the greater stability derived from side-on co-ordination compared to end-on bonding of CH_2O. This emphasizes that co-ordination preferably occurs to electron-rich rather than to acidic metals.

The purpose of the present paper is to provide a theoretical *'ab initio'* interpretation of the co-ordinate bond between iron and formaldehyde, conducted at both Hartree–Fock and post-Hartree–Fock configuration-interaction levels of approximation. Three formaldehyde complexes, $[Fe(CO)_2(PH_3)_2(\eta^2\text{-}CH_2O)]$, $[Fe(CO)_4(\eta^2\text{-}CH_2O)]$, and $[Fe(PH_3)_4(\eta^2\text{-}CH_2O)]$, have been examined. The first can be assumed as a model for $[Fe(CO)_2\{P(OMe)_3\}_2(\eta^2\text{-}CH_2O)]$, a species well characterized experimentally,[7] and with particular relevance given to the catalytic activity of iron in the Fischer–Tropsch synthesis.[1] The phosphines PH_3 and $P(OMe)_3$ differ significantly because of their donor ability to the metal, but our major goal was to observe a trend parallel to the stepwise ligand substitution at the metal. The tetracarbonyl and tetrakis(phosphine) species are not models for real complexes, but are studied here to investigate the effects of ligand substitution and metal basicity on the binding of formaldehyde. For this purpose, we have mainly analysed the energetics of the variations of CH_2O binding to iron in the series $[Fe(CO)_{4-n}(PH_3)_n(\eta^2\text{-}CH_2O)]$, with *n* = 0, 2, or 4.

Computation

Basis Sets.—Two Gaussian basis sets, hereafter denoted as I and II, were employed throughout this work. In basis I, the functions for iron were derived from Huzinaga's MINI-4 basis[9] by splitting the outermost *s* and *d* functions. The MINI-1 basis[10,11] was used for the phosphorus atoms and the carbonyl groups, and a (2*s*) contraction[10] of Van Duijneveldt's (4*s*) primitive set[12] was adopted for the phosphine hydrogens. For the component atoms of formaldehyde, Dunning's basis set[13] of double-zeta quality was employed. All geometry optimizations described herein were conducted using this basis. Subsequent single-point self-consistent field and configuration interaction calculations at the optimized geometries were performed using the more extended basis II. Here the *s,p* basis for iron was taken from the (12*s*6*p*4*d*) set of ref. 14 with the addition of two basis functions to describe the 4*p* orbital,[15] while the Fe *d* basis was the reoptimized (5*d*) set of ref. 16, contracted (4/1). This leads to an (11*s*8*p*5*d*) primitive basis for iron, contracted (8*s*6*p*2*d*). A double-zeta expansion was used for all ligand atoms, with a (4*s*/2*s*) basis for H,[13] a (9*s*5*p*/4*s*2*p*) contraction for carbon and oxygen,[13] and an (11*s*7*p*/6*s*4*p*) contraction for phosphorus.[17]

The basis set superposition error, as proposed by Boys and Bernardi,[18] was calculated for the complex $[Fe(CO)_2(PH_3)_2(\eta^2\text{-}CH_2O)]$. Basis I and basis II values of 3.9 and 4.6 kcal mol^{-1}, respectively, suggest that our results should not be unduly affected by superposition errors.

Methods.—Two levels of theory were employed for studying the ground states of the three complexes investigated, the fragments $Fe(CO)_2(PH_3)_2$, $Fe(CO)_4$, and $Fe(PH_3)_4$, and formaldehyde itself. *'Ab initio'* spin-restricted Hartree–Fock gradient calculations were used in partial geometry optimizations of the three complexes and in deriving estimates of the binding energies of all complexes with respect to free CH_2O and fragment species. Single reference-state configuration-interaction calculations [hereafter referred to as single plus double configuration interaction (s.d.c.i.)] were subsequently performed on the tetracarbonyl complex and associated fragments, including single and double excitations from the upper valence orbitals using the direct configuration-interaction method.[19] With 29 'frozen' orbitals and 40 active electrons in the complex, excitations to the lowest 77 virtual orbitals of the basis II self-consistent field wavefunction led to a configuration-interaction expansion of 595 091 configurations. A consistent approach to freezing and discarding of orbitals in the $^1A_1$ states of $Fe(CO)_4$

---

† *Non-S.I. units employed:* cal = 4.184 J, hartree ≈ 4.36 × 10^{-18} J.

and CH_2O led to configuration spaces of 128 145 and 471 respectively, with 25 frozen and 14 discarded orbitals in $Fe(CO)_4$, and four frozen and two discarded orbitals in formaldehyde.

All computations were performed using the GAMESS program package[20] implemented on the cluster of FPS-164 processors at the IBM European Center for Scientific and Engineering Computing (ECSEC, Rome).

Geometries and Geometry Optimization.—In all the calculations described herein we have confined our attention to geometries involving side-on co-ordination of the formaldehyde; such an approach is consistent with the experimental evidence that no end-on complex has so far been isolated. Moreover such a bonding mode requires an electron-rich metal. The geometries of the complexes used in initial basis I self-consistent field studies were derived from the structure of $[Fe(CO)_2\{P(OMe)_3\}_2(\eta^2\text{-}CH_2O)]$ reported by Berke *et al.*[7b] With the iron atom bonded to two mutually *trans* trimethyl phosphites, two carbonyls, and the formaldehyde, the nature of the interaction with CH_2O allows the complex to be viewed as either a distorted trigonal bipyramid, with a five-co-ordinated iron atom, or a distorted octahedron, with a six-co-ordinated iron atom. The former description arises from a unidentate formaldehyde, the latter from a bidentate interaction. Given the side-on co-ordination of CH_2O, together with the angle of 103.2° formed by the iron with the equivalent carbonyls, the structure is best regarded as a distorted octahedron.[7b] In the model system $[Fe(CO)_2(PH_3)_2(\eta^2\text{-}CH_2O)]$, the geometry of the $Fe(CO)_2(PH_3)_2$ fragment was taken from ref. 7*b* and idealized to C_{2v} symmetry, a not over severe approximation given the small deviations from such in the experimental structure. The geometry of the phosphine ligands was taken from ref. 21.

A general feature of $M\text{-}CH_2O$ complexes appears to be the asymmetry of the co-ordinated formaldehyde in the side-on mode; the experimental Fe–C and Fe–O distances in the trimethyl phosphite complex are 2.00 and 2.03 Å respectively. This asymmetry was thus included in the model system. The formaldehyde C–H distance and HCH bond angle were set to the values of the free molecule,[22] while the C–O distance was taken from the experimental structure of the complex. This is justified by most of the complexes previously reported, except for the osmium complex $[Os(CO)_2(PPh_3)_2(\eta^2\text{-}CH_2O)]$.[3] Figure 1 shows the structure of the resulting 'fixed geometry' model system.

In the absence of experimental information for the tetracarbonyl and tetrakis(phosphine) complexes, molecular geometries were based on the model system above. In substituting the axial phosphines, a $C_{ax}\text{-}Fe\text{-}C_{ax}$ angle of 180° was assumed for the tetracarbonyl, and likewise the experimental $C_{eq}\text{-}Fe\text{-}C_{eq}$ angle was used when substituting the equatorial carbonyls to yield the tetrakis(phosphine) complex.

To investigate the asymmetry of the co-ordinated CH_2O further, we performed partial geometry optimizations of the three complexes. With the iron-fragment geometry fixed at the model values above, the geometrical parameters of the co-ordinated CH_2O were optimized subject to the side-on constraint of the bonded formaldehyde.

In considering the electronic structures of the isolated fragments, $Fe(CO)_4$, $Fe(CO)_2(PH_3)_2$, and $Fe(PH_3)_4$, the geometries were taken to be equal to those in the formaldehyde complexes. Dissociation to these fragments may lead to either singlet or triplet products. The singlet–triplet splitting of the formaldehyde molecule is known experimentally to be 71.9 kcal mol^{-1}.[23] Basis I self-consistent field calculations on the fragments predict the $^3B_1$ state to be more stable than the $^1A_1$, by 41.2, 53.8, and 66.9 kcal mol^{-1} for $Fe(CO)_4$, $Fe(CO)_2(PH_3)_2$, and $Fe(PH_3)_4$ respectively. These splittings, although in agreement with magnetic circular dichroism measurements performed on $Fe(CO)_4$, in an argon matrix, which showed its paramagnetism,[24] are, however, clearly overestimated. Basis II self-consistent field calculations on iron tetracarbonyl reduce the separation to 24.9 kcal mol^{-1}. Inclusion of correlation effects, through single reference s.d.c.i. calculations, predictably reduces the splitting still further, given the greater correlation energy of the closed-shell singlet state. The s.d.c.i. splitting of 8.9 kcal mol^{-1} is reduced to 4.4 kcal mol^{-1} when including the effects of higher excitations through the Davidson correction.[25] While these calculations do not allow a definitive assignment of the ground state of the fragment species, they do allow us to suggest with some confidence that fragmentation of the complexes will lead to singlet products, given the $S_0 \longrightarrow T_1$ value of 71.9 kcal mol^{-1} in free formaldehyde. Consequently, the theoretical

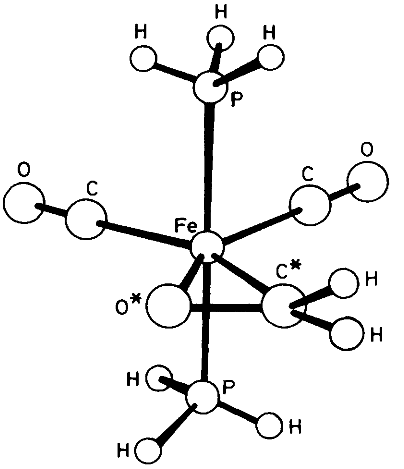

Figure 1. Fixed geometry of the model system $[Fe(CO)_2(PH_3)_2(\eta^2\text{-}CH_2O)]$. Selected bond lengths (Å) and angles (°) are as follows: Fe–P 2.21, Fe–C 1.76, C–O 1.13, Fe–C* 2.03, Fe–O* 2.00, C*–O* 1.32, and C*–H 1.12; Fe–C–O 177.0; C–Fe–C 103.2, P–Fe–P 177.9, O*–Fe–C* 38.2, C*–Fe–C 108.5, and H–C*–H 116.5

Table 1. Total self-consistent field energies (hartree) with binding energies (kcal mol^{-1}) in parentheses

	Basis I		Basis II
Complex or fragment	Fixed geometry	Optimized geometry	Optimized geometry
$[Fe(CO)_4(\eta^2\text{-}CH_2O)]$	−1 819.0684 (−8.2)	−1 819.0806 (−15.9)	−1 826.5276 (−22.6)
$[Fe(CO)_2(PH_3)_2(\eta^2\text{-}CH_2O)]$	−2 276.6878 (−20.8)	−2 276.7033 (−30.5)	−2 285.9449 (−32.8)
$[Fe(PH_3)_4(\eta^2\text{-}CH_2O)]$	−2 734.2911 (−44.7)	−2 734.3141 (−59.2)	−2 745.3397 (−70.4)
$Fe(CO)_4$	−1 705.2260		−1 712.6623
$Fe(CO)_2(PH_3)_2$	−2 162.8254		−2 172.0633
$Fe(PH_3)_4$	−2 620.3905		−2 631.3982
CH_2O	−113.8293		−113.8293

results which will be discussed in the following sections refer to the lowest singlet states of the molecular species investigated.

Results and Discussion

Study of the Iron–Formaldehyde Bond.—The total self-consistent field energies of the complexes and fragments under investigation, together with estimates of the binding energies, are reported in Table 1. Partially optimized structures of the complexes are shown in Table 2. In Table 3 we show the energy and atomic orbital character of the upper valence molecular orbitals for each of the complexes.

Table 2. Optimized geometries of the systems under investigation. Bond lengths in Å, angles in °

	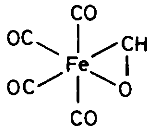	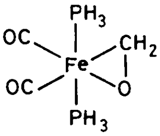	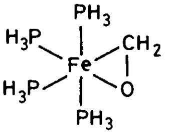
Fe–C	2.097	1.952 (2.03)[a]	1.900
Fe–O	2.055	1.971 (2.00)[a]	1.917
C–O	1.262	1.311 (1.32)[a]	1.354
C–Fe–L[b]	104.6	102.1 (108.5)[a]	110.1
C–H	1.080	1.082	1.087
H–C–H	115.1	112.4	110.5
α[c]	16.1	29.1	37.3

[a] Experimental value relative to $[Fe(CO)_2\{P(OMe)_3\}_2(\eta^2\text{-}CH_2O)]$. [b] L = CO in $[Fe(CO)_4(\eta^2\text{-}CH_2O)]$ and $[Fe(CO)_2(PH_3)_2(\eta^2\text{-}CH_2O)]$, PH_3 in $[Fe(PH_3)_4(\eta^2\text{-}CH_2O)]$. [c] Distortion angle defined as the angle between the CH_2 plane and the C–O bond.

The co-ordination of CH_2O by the iron complex can occur either by addition of CH_2O to the unsaturated species (**1**) [reaction (2)] generated by thermal or photochemical labilization of the ligand L [reaction (1)], or by substitution of L by CH_2O [reaction (3)]. The binding (or interaction) energy we are discussing is referred to the addition of CH_2O to the high-energy fragment (**1**), $\Delta E = E[Fe(CO)_2(PH_3)_2(\eta^2\text{-}CH_2O)] - E[Fe(CO)_2(PH_3)_2] - E(CH_2O)$, and is computed to be -20.8 kcal mol^{-1} (basis I). The terms $E[Fe(CO)_2(PH_3)_2(\eta^2\text{-}CH_2O)]$ and $E[Fe(CO)_2(PH_3)_2]$ are the complex and fragment energies in the model geometry detailed in the previous section, while $E(CH_2O)$ is the formaldehyde energy at its equilibrium geometry; ΔE does not tell us whether we can make the compound or not, unless we are able to generate the unsaturated species 'Fe(CO)$_2$(PH$_3$)$_2$,' *e.g.* thermally or photochemically, *etc.*

$$[Fe(CO)_2(PH_3)_2L] \xrightarrow{h\nu \text{ or heat}} \text{'}Fe(CO)_2(PH_3)_2\text{'} + L \qquad (1)$$

(1)

$$\text{'}Fe(CO)_2(PH_3)_2\text{'} + CH_2O \longrightarrow [Fe(CO)_2(PH_3)_2(CH_2O)] \qquad (2)$$

(2)

$$[Fe(CO)_2(PH_3)_2L] + CH_2O \longrightarrow [Fe(CO)_2(PH_3)_2(CH_2O)] + L \qquad (3)$$

(2)

Table 3. Upper valence molecular obitals

			Population analysis (%)			
Complex	Orbital	Energy (hartree)	Fe	CH_2O	Axial ligands	Equatorial ligands
$[Fe(CO)_4(\eta^2\text{-}CH_2O)]$					CO	CO
	34*a*′	−0.3165	50	26	6	18
	15*a*″	−0.4330	3	97		
	33*a*′	−0.4405	47	40	2	11
	14*a*″	−0.5286	82	4	10	4
	32*a*′	−0.5293	28	58		4
	13*a*″	−0.5494	77	8	12	3
$[Fe(CO)_2(PH_3)_2(\eta^2\text{-}CH_2O)]$					PH_3	CO
	36*a*′	−0.2582	47	33	2	18
	17*a*″	−0.3884	2	90	8	
	35*a*′	−0.4010	46	41	2	11
	16*a*″	−0.4197	2	9	86	3
	34*a*′	−0.4390	14	4	74	8
	33*a*′	−0.4944	35	51	8	6
	15*a*″	−0.4966	74		24	2
	14*a*″	−0.5090	62	1	36	2
$[Fe(PH_3)_4(\eta^2\text{-}CH_2O)]$					PH_3	PH_3
	38*a*′	−0.2003	46	43	2	9
	19*a*″	−0.3377	3	95	2	
	37*a*′	−0.3621	34	34	6	26
	36*a*′	−0.3825	14	18	48	20
	18*a*″	−0.3883	2	6	88	4
	35*a*′	−0.4177	12	1	4	83
	34*a*′	−0.4493	46	40	4	10
	17*a*″	−0.4493	87	1	8	4
	16*a*″	−0.4658	80	3	14	3

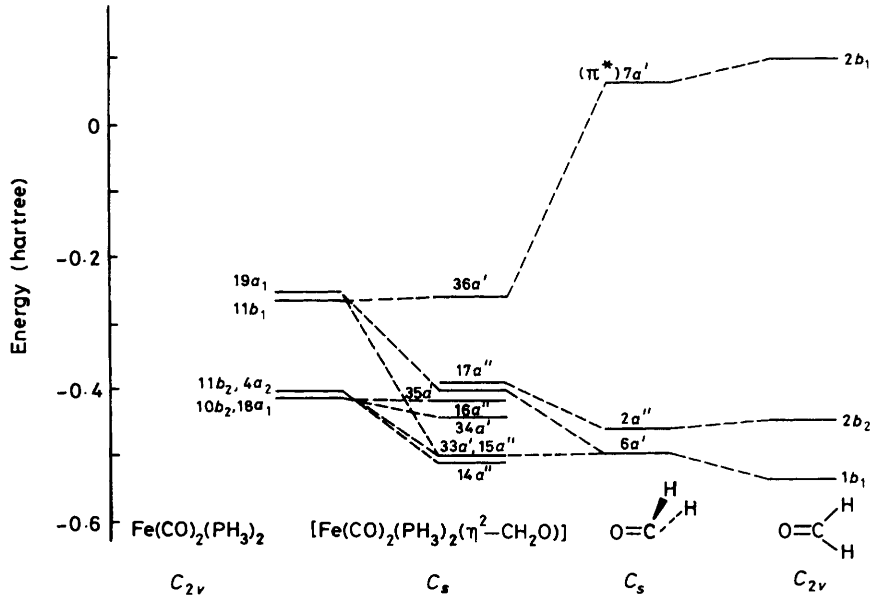

Figure 2. Molecular-orbital correlation diagram of $[Fe(CO)_2(PH_3)_2(\eta^2-CH_2O)]$

The distortion of the formaldehyde molecule upon co-ordination is seen to be satisfactorily reproduced in the optimized structure of Table 2. In particular, the elongation of the C–O distance on bonding, from 1.21 to 1.32 Å, is accurately predicted (1.311 Å in the optimized structure), while the distortion angle, defined as the angle between the CH_2 plane and the C–O bond, is calculated to be 29.1°. This value is in line with the experimental angle of 26.6° found in the complex $[Ni(PEt_3)_2(\eta^2-CPh_2O)]$.[26] The iron–formaldehyde bond is experimentally found to be very slightly asymmetric, with the Fe–C distance (2.03 Å) longer than the Fe–O distance (2.00 Å). Our partially optimized structure satisfactorily reproduces the absolute values of these bond distances (1.952 Å for Fe–C and 1.971 Å for Fe–O), although the slightly greater deviation from experiment of the Fe–C distance causes an inversion in their relative magnitude. The calculated C–Fe–O angle of 39.0° is in excellent agreement with the experimental estimate of 38.2°.

The optimization of the complex geometry increases the basis I binding energy to -30.5 kcal mol^{-1}, although we stress again that this value is with respect to the frozen geometry fragment $Fe(CO)_2(PH_3)_2$. The basis II estimate, using the optimized geometry above, is -32.8 kcal mol^{-1}.

The analysis of Table 3 shows that the molecular orbitals (m.o.s) involved in iron–formaldehyde bonding are the 33*a*′, 35*a*′, and 36*a*′. Correlating the m.o.s of the fragments provides a useful way of interpreting the nature and origin of the Fe–CH_2O bond. Figure 2 shows such a correlation diagram of the orbitals of $[Fe(CO)_2(PH_3)_2(\eta^2-CH_2O)]$ with those of the singlet fragments, where only the main correlations are reported. The 33*a*′ and 35*a*′ m.o.s are respectively the bonding and antibonding combination of the formaldehyde $1b_1$–π orbital and the $Fe(CO)_2(PH_3)_2$ $19a_1$ m.o., which is predominantly iron d_{z^2} in character. The 36*a*′ m.o., the highest occupied molecular orbital, is the bonding combination of the formaldehyde $2b_1$–π* and the fragment $11b_1$, which is mainly Fe–d_{xz}. Clearly the main interaction between the iron and the formaldehyde is the π-back donation from the transition metal to the ligand, while the $CH_2O \rightarrow Fe$ donation is almost absent. This picture is substantiated on performing a localization of the molecular orbitals using the Foster–Boys algorithm.[27] The resulting localized molecular orbitals (l.m.o.s) reveal that effective bonding between iron and formaldehyde is concentrated in a single l.m.o., featuring overlap of the metal $3d_{xz}$ and the antibonding π component of the CH_2O basis orbitals.

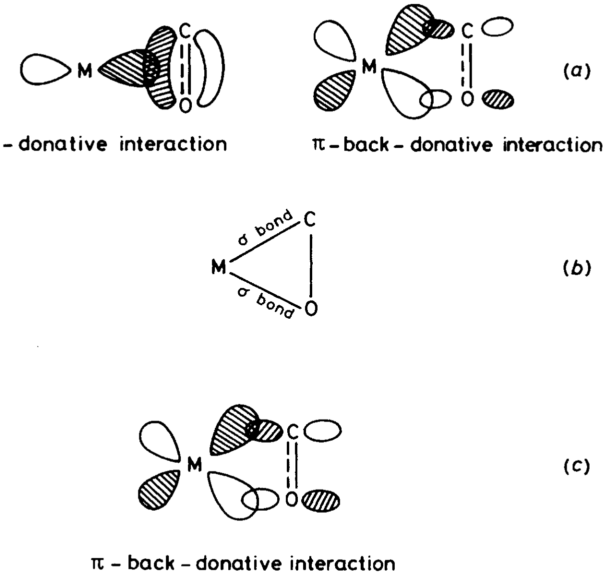

Figure 3. Bonding models for the side-on co-ordination of CH_2O to a metal fragment: (*a*) Chatt–Dewar–Duncanson; (*b*) metallacyclopropane; (*c*) present

Those facts lead to the conclusion that the interaction of CH_2O with iron(0) in fragment (**1**) can be described neither by the classic Chatt–Dewar–Duncanson model[28] nor by a metallacyclopropane structure,[29] since both models require the utilization of two orbitals from the metal for bonding CH_2O (Figure 3).

The back donation of electron density from filled metal *d* orbitals into empty π* orbitals of an unsaturated molecule implies a lengthening of the multiple bond of the unsaturated molecule. This is evident in the case under investigation since the C–O distance increases from 1.21 Å (in the free

Table 4. Mulliken population analysis of $[Fe(CO)_4(\eta^2\text{-}CH_2O)]$, $[Fe(CO)_2(PH_3)_2(\eta^2\text{-}CH_2O)]$, $[Fe(PH_3)_4(\eta^2\text{-}CH_2O)]$ and the separated fragments

	Fe			CH_2O			Axial ligands	Equatorial ligands
Complex or fragments	*s*	*p*	*d*	C	O	H_2	CO	CO
$Fe(CO)_4 + CH_2O$	6.28	12.53	7.32	5.99	8.31	1.70	27.88	27.99
$[Fe(CO)_4(\eta^2\text{-}CH_2O)]$	6.34	12.60	7.24	6.09	8.44	1.68	27.77	27.84
							PH_3	CO
$Fe(CO)_2(PH_3)_2 + CH_2O$	6.26	12.64	7.23	5.99	8.31	1.70	35.61	28.26
$[Fe(CO)_2(PH_3)_2(\eta^2\text{-}CH_2O)]$	6.35	12.65	7.17	6.17	8.55	1.75	35.48	27.88
							PH_3	PH_3
$Fe(PH_3)_4 + CH_2O$	6.17	12.24	7.62	5.99	8.31	1.70	35.86	36.11
$[Fe(PH_3)_4(\eta^2\text{-}CH_2O)]$	6.33	12.51	7.15	6.29	8.64	1.83	35.66	35.59

Table 5. Details and results of the configuration-interaction calculations on $[Fe(CO)_4(\eta^2\text{-}CH_2O)]$

	$Fe(CO)_4$			$[Fe(CO)_4(\eta^2\text{-}CH_2O)]$	
	Basis I	Basis II	CH_2O*	Basis I	Basis II
No. of active electrons	32	32	8	40	40
No. of active orbitals	38	79	18	56	97
No. of configurations	15 825	128 145	471	145 433	595 091
Energy fixed geometry (hartree)	−1 705.8017	−1 713.4186	−113.9706	−1 819.7917	
Energy optimized geometry (hartree)				−1 819.7971	−1 827.4071
	Fixed geometry Basis I		Optimized geometry Basis I	Optimized geometry Basis II	
Binding energy (kcal mol^{-1})	−12.2		−15.6	−11.2	

* For CH_2O, basis I = basis II.

formaldehyde) to 1.32 Å (in the complex). In Table 4 we have collected the Mulliken populations of the complexes and fragments studied. Since π-back donation is the main source of interaction between iron and CH_2O in $[Fe(CO)_2(PH_3)_2(\eta^2\text{-}CH_2O)]$, the increase in formaldehyde population of 0.47 electrons upon co-ordination can be taken as a direct estimate of the amount of such π-back donation.

The Mulliken population allows an oxidation state to be assigned which is significantly different from the formal one, which foresees either +2 and −2 for iron and CH_2O respectively, or zero for both. Data from Table 4 confirm that oxygen is, as in free formaldehyde, more nucleophilic than carbon in the co-ordinated formaldehyde. From Table 4 we can also observe that the carbonyl groups show, as expected, an electron-acceptor character, which decreases as the formaldehyde binds, while the phosphine groups exhibit a weak electron-donor character.

Ligand Influence.—The binding energies of the compounds $[Fe(CO)_4(\eta^2\text{-}CH_2O)]$ and $[Fe(PH_3)_4(\eta^2\text{-}CH_2O)]$, in the model geometries previously detailed, are computed with basis I to be −8.2 and −44.7 kcal mol^{-1}, respectively (see Table 1). The optimization of the geometries of the complexes increases the basis I binding energy to −15.9 and −59.2 kcal mol^{-1}. The basis II estimates, using the optimized geometries, are −22.6 and −70.4 kcal mol^{-1}. The replacement of carbonyl ligands with phosphines implies therefore an increase in the binding energy.

The partially optimized geometries of the analysed systems, Table 2, show that the distortion of the formaldehyde molecule upon co-ordination increases with the substitution of carbonyl ligands with phosphines, suggesting the presence of a stronger interaction with the transition metal. In particular, the C–O distance, which is 1.262 Å in the tetracarbonyl compound, becomes 1.311 Å in the dicarbonyldiphosphine system and 1.354 Å in the tetrakis(phosphine) compound, while the distortion angle, defined as the angle between the CH_2 plane and the C–O bond, is calculated to be 16.1, 29.1, and 37.3° in $[Fe(CO)_4(\eta^2\text{-}CH_2O)]$, $[Fe(CO)_2(PH_3)_2(\eta^2\text{-}CH_2O)]$, and $[Fe(PH_3)_4(\eta^2\text{-}CH_2O)]$, respectively. Moreover, the distance between the iron fragment and the formaldehyde molecule decreases upon replacement of carbonyls with phosphines, confirming the presence of a stronger bond in the tetrakis(phosphine) compound.

Table 3, which collects the Mulliken populations for the valence orbitals, shows that the orbitals involved in the iron–formaldehyde bonding are the 32*a*′, 33*a*′, and 34*a*′ for $[Fe(CO)_4(\eta^2\text{-}CH_2O)]$ and the 34*a*′, 37*a*′, and 38*a*′ for $[Fe(PH_3)_4(\eta^2\text{-}CH_2O)]$. The first two orbitals are the bonding and the antibonding combination of the formaldehyde π orbital and the fragment orbital with mainly Fe–d_{z^2} character. The third orbital, which is the highest occupied molecular orbital, is the bonding combination of the formaldehyde π* orbital and the fragment orbital with predominantly Fe–d_{xz} character. Therefore also for the compounds $[Fe(CO)_4(\eta^2\text{-}CH_2O)]$ and $[Fe(PH_3)_4(\eta^2\text{-}CH_2O)]$, the main bonding interaction is the π-back donation from the metal to the unsaturated ligand. The localized molecular orbitals confirm that effective bonding between iron and formaldehyde is concentrated in a single l.m.o, which is essentially the combination of metal d_{xz} and formaldehyde antibonding π orbitals.

The chemical conclusion is that we need to transfer electrons to CH_2O (*i.e.* to reduce CH_2O) in order to bind it, and this occurs *via* a single metal orbital. Moreover, the presence of electron-acceptor ligands such as carbonyl decreases the electron density at the iron atom, hence the back donation and therefore the strength of the interaction between Fe and CH_2O. Indeed, from Table 4, the increase in formaldehyde Mulliken population upon co-ordination is 0.21 for $[Fe(CO)_4(\eta^2\text{-}CH_2O)]$, 0.47 for $[Fe(CO)_2(PH_3)_2(\eta^2\text{-}CH_2O)]$, and 0.76 for $[Fe(PH_3)_4(\eta^2\text{-}CH_2O)]$. This shows that the π-back donation increases upon replacing the carbonyls with phosphines. This increases the strength of the iron–formaldehyde bond, as is suggested by the binding energy, which is -22.6, -32.8, and -70.4 kcal mol^{-1} along the series we are discussing.

The ligand influence can be explained in a different way by considering the energy of the fragment orbital with mainly Fe–d_{xz} character, which lies at -0.3249 hartree in $Fe(CO)_4$, at -0.2657 hartree in $Fe(CO)_2(PH_3)_2$, and at -0.1647 hartree in $Fe(PH_3)_4$. Since the formaldehyde π^*-orbital energy is 0.1077 hartree, the replacement of CO with PH_3 decreases the gap between the CH_2O π^* and the fragment orbital of mainly Fe–d_{xz} character: hence the overlap increases.

Configuration-interaction Calculations on the Complex $[Fe(CO)_4(\eta^2\text{-}CH_2O)]$.—To check the influence of correlation energy on the analysis performed, single reference s.d.c.i. calculations have been carried out on the compound $[Fe(CO)_4(\eta^2\text{-}CH_2O)]$, by using the direct configuration-interaction method.[19] The basis sets employed are the same as in the self-consistent field calculations. Fifty-eight electrons have been frozen because of the dimensions of the problem (49 doubly occupied orbitals and 142 basis functions using the bigger basis set). In the evaluation of the energies of $Fe(CO)_4$ and CH_2O, the orbitals correlating with those frozen and discarded in the complex have themselves been frozen and discarded. The self-consistent field ground-state configuration was chosen as the reference function and all possible single and double excitations were included, except those from the frozen core orbitals.

Table 5 shows the details and results of the configuration-interaction calculations on the complex and the separated fragments. The Davidson correction[25] was always added to correct for the lack of size consistency of the wavefunction. The binding energy is computed to be -12.2 kcal mol^{-1}, using basis I and the fixed geometry of the complex, and -15.6 and -11.2 kcal mol^{-1} at the optimized geometry, using basis I and II, respectively. These results show that correlation effects are particularly relevant in the basis II calculation and they seem to be more important for the fragment species than for the complex. Indeed the basis II binding energy at the configuration-interaction level is smaller than that computed at the Hartree–Fock level, while the configuration-interaction and self-consistent field binding energies computed with basis I are comparable. However, since the difference between these binding energies is small, we can conclude with some confidence that the energetics of bond formation between Fe and CH_2O is not markedly affected by correlation effects.

Conclusions

An '*ab initio*' theoretical study of the compound $[Fe(CO)_2\{P(OMe)_3\}_2(\eta^2\text{-}CH_2O)]$ has been carried out through the use of the model system $[Fe(CO)_2(PH_3)_2(\eta^2\text{-}CH_2O)]$ which contains all the fundamental features of the experimental system. The energetics of co-ordination of a formaldehyde molecule to a transition metal has been investigated, showing that the main interaction is π-back donation from the metal to the unsaturated molecule.

The study of the systems $[Fe(CO)_4(\eta^2\text{-}CH_2O)]$ and $[Fe(PH_3)_4(\eta^2\text{-}CH_2O)]$, as models for compounds not yet synthesized, has shown that the increase in number of electron-acceptor carbonyl ligands decreases the back donation. Indeed the Fe–CH_2O interaction in $[Fe(CO)_4(\eta^2\text{-}CH_2O)]$ is fairly weak, while $[Fe(PH_3)_4(\eta^2\text{-}CH_2O)]$ shows a quite strong bond. An analysis of the electron distribution, computed *via* Mulliken population analysis, supports the above results. Upon co-ordination, the electron density on formaldehyde increases and that on the iron *d* orbitals decreases. Also, the electron density on formaldehyde increases on going from $[Fe(CO)_4(\eta^2\text{-}CH_2O)]$ to $[Fe(PH_3)_4(\eta^2\text{-}CH_2O)]$.

The configuration-interaction calculations carried out on the complex $[Fe(CO)_4(\eta^2\text{-}CH_2O)]$ have clarified that the correlation effects, although relevant to the description of this system, do not markedly affect the energetics of bond formation between Fe and CH_2O, so that the interaction energies computed at the Hartree–Fock level appear to be reliable.

Acknowledgements

Thanks are due to the IBM European Center for Scientific and Engineering Computing (ECSEC, Rome) for provision of computing facilities and visiting grants. Support by the Italian National Research Council (CNR), the Ministry of Public Education (MPI), and the Petroleum Research Fund of the American Chemical Society (Grant PRF17464-AC3) is greatly acknowledged. M. F. G. Thanks the British Council for a travel grant.

References

1 G. Henrici-Olivé and S. Olivé, *Angew. Chem., Int. Ed. Engl.*, 1976, **15**, 136; E. L. Muetterties and J. Stein, *Chem. Rev.*, 1979, **79**, 479; C. K. Rofer-DePoorter, *ibid.*, 1981, **81**, 447; W. A. Herrmann, *Angew. Chem., Int. Ed. Engl.*, 1982, **21**, 117.

2 K. L. Brown, G. R. Clark, C. E. L. Headford, K. Marsden, and W. R. Roper, *J. Am. Chem. Soc.*, 1979, **101**, 503; T. B. Rauchfuss, *ibid.*, p. 1045; B. D. Dombek, *ibid.*, 1980, **102**, 6855; D. R. Fahey, *ibid.*, 1981, **103**, 136; J. A. Gladysz, *Adv. Organomet. Chem.*, 1982, **20**, 1; J. R. Blackborow, R. J. Daroda, and G. Wilkinson, *Coord. Chem. Rev.*, 1982, **43**, 17.

3 G. R. Clark, C. E. L. Headford, K. Marsden, and W. R. Roper, *J. Organomet. Chem.*, 1982, **231**, 335.

4 S. Gambarotta, C. Floriani, A. Chiesi-Villa, and C. Guastini, *J. Am. Chem. Soc.*, 1982, **104**, 2019; *Organometallics*, 1986, **5**, 2425.

5 S. Gambarotta, C. Floriani, A. Chiesi-Villa, and C. Guastini, *J. Am. Chem. Soc.*, 1985, **107**, 2985.

6 W. E. Buhro, A. T. Patton, C. E. Strouse, J. A. Gladysz, F. B. McCormick, and M. C. Etter, *J. Am. Chem. Soc.*, 1983, **105**, 1056.

7 (*a*) H. Berke, W. Bankhardt, G. Huttner, J. v. Seyerl, and L. Zsolnai, *Chem. Ber.*, 1981, **114**, 2754; (*b*) H. Berke, G. Huttner, G. Weiler, and L. Zsolnai, *J. Organomet. Chem.*, 1981, **219**, 353.

8 S. Sakaki, K. Kitaura, K. Morokuma, and K. Ohkubo, *Inorg. Chem.*, 1983, **22**, 104.

9 H. Tatewaki, Y. Sakai, and S. Huzinaga, *J. Comput. Chem.*, 1981, **2**, 278.

10 H. Tatewaki and S. Huzinaga, *J. Comput. Chem.*, 1980, **1**, 205.

11 Y. Sakai, H. Tatewaki, and S. Huzinaga, *J. Comput. Chem.*, 1981, **2**, 100.

12 F. B. Van Duijneveldt, IBM Research Report, 1971, RJ, p. 945.

13 T. H. Dunning, jun., *J. Chem. Phys.*, 1970, **53**, 2823.

14 R. Roos, A. Veillard, and G. Vinot, *Theor. Chim. Acta*, 1971, **20**, 1.

15 D. M. Hood, R. M. Pitzer, and H. F. Schaefer III, *J. Chem. Phys.*, 1979, **71**, 705.

16 A. K. Rappe, T. A. Smedley, and W. A. Goddard III, *J. Phys. Chem.*, 1981, **85**, 2607.

17 T. H. Dunning, jun., and P. J. Hay, in 'Modern Theoretical Chemistry,' ed. H. F. Schaefer III, Plenum, New York, 1977, vol. 4, p. 1.

18 S. F. Boys and F. Bernardi, *Mol. Phys.*, 1970, **19**, 553.

19 V. R. Saunders and J. H. Van Lenthe, *Mol. Phys.*, 1983, **48**, 923.

20 M. Dupuis, D. Spangler, and J. Wendolowski, NRCC Software Catalog, vol. 1, Program N. QG01 (GAMESS), 1980; M. F. Guest and J. Kendrick, GAMESS User Manual, Technical Memorandum, SERC Daresbury Laboratory, 1985.

21 E. Sutton, 'Tables of Interatomic Distances and Configuration in Molecules and Ions,' Chemical Society, London, 1958.

22 T. Oka, *J. Phys. Soc. Jpn.*, 1960, **15**, 2274.

23 G. Herzberg, 'Electronic Spectra and Electronic Structure of Polyatomic Molecules,' Van Nostrand, Princeton, 1966.

24 T. J. Barton, R. Grinter, A. J. Thomson, B. Davies, and M. Poliakoff, *J. Chem. Soc., Chem. Commun.*, 1977, 841.

25 E. R. Davidson, in 'The World of Quantum Chemistry,' eds. R. Daudel and B. Pullman, Reidel, Dordrecht, 1974.

26 T. T. Tsou, J. C. Huffman, and J. K. Kochi, *Inorg. Chem.*, 1979, **18**, 2311.

27 J. M. Foster and S. F. Boys, *Rev. Mod. Phys.*, 1960, **32**, 300.

28 M. J. S. Dewar, *Bull. Soc. Chim. Fr.*, 1951, **18c**, 71; J. Chatt and J. A. Duncanson, *J. Chem. Soc.*, 1953, 2939.

29 P. Conway, S. M. Grant, and A. R. Manning, *J. Chem. Soc., Dalton Trans.*, 1979, 1920.

Received 9th February 1987; Paper 7/232